



HAL
open science

Electrical and physical topography in energy-filtered photoelectron emission microscopy of two-dimensional silicon pn junctions

Maylis Lavayssière, Matthias Escher, Olivier Renault, Denis Mariolle,
Nicholas Barrett

► **To cite this version:**

Maylis Lavayssière, Matthias Escher, Olivier Renault, Denis Mariolle, Nicholas Barrett. Electrical and physical topography in energy-filtered photoelectron emission microscopy of two-dimensional silicon pn junctions. *Journal of Electron Spectroscopy and Related Phenomena*, 2013, 186, pp.30 - 38. 10.1016/j.elspec.2013.01.014 . cea-01477558

HAL Id: cea-01477558

<https://cea.hal.science/cea-01477558>

Submitted on 27 Sep 2017

HAL is a multi-disciplinary open access archive for the deposit and dissemination of scientific research documents, whether they are published or not. The documents may come from teaching and research institutions in France or abroad, or from public or private research centers.

L'archive ouverte pluridisciplinaire **HAL**, est destinée au dépôt et à la diffusion de documents scientifiques de niveau recherche, publiés ou non, émanant des établissements d'enseignement et de recherche français ou étrangers, des laboratoires publics ou privés.



Electrical and physical topography in energy-filtered photoelectron emission microscopy of two-dimensional silicon pn junctions

Maylis Lavayssière^a, Matthias Escher^b, Olivier Renault^a, Denis Mariolle^a, Nicholas Barrett^{c,*}

^a CEA, LETI, MINATEC Campus, 17 rue des Martyrs, 38054 Grenoble Cedex 9, France

^b Focus GmbH, 65510 Hünstetten, Germany

^c CEA, IRAMIS/SPCSI/LENSIS, F-91191 Gif-sur-Yvette, France

ARTICLE INFO

Article history:

Received 17 May 2012

Received in revised form 7 January 2013

Accepted 17 January 2013

Available online 12 February 2013

Keywords:

Pn junction

Photoelectron emission microscopy

Surface imaging

Simulations

ABSTRACT

Photoelectron emission microscopy (PEEM) is a powerful non-destructive tool for spatially resolved, spectroscopic analysis of surfaces with sub-micron chemical heterogeneities. However, in the case of micron scale patterned semiconductors, band line-ups at pn junctions have a built-in lateral electric field which can significantly alter the PEEM image of the structure with respect to its physical dimensions. Furthermore, real surfaces may also have physical topography which can reinforce or counteract the electrically induced distortion at a pn junction. We have measured the experimental PEEM image distortion at such a junction and carried out numerical simulations of the PEEM images. The simulations include energy filtering and the use of a contrast aperture in the back focal plane in order to describe the changes in the PEEM image of the junction with respect to its real physical dimensions. Threshold imaging does not give a reliable measurement of micron sized p and n type patterns. At higher take-off energies, for example using Si 2p electrons, the pattern width is closer to the real physical size. Physical topography must also be quantitatively accounted for. The results can be generalized to PEEM imaging of any structure with a built-in lateral electric field.

© 2013 Elsevier B.V. All rights reserved.

1. Introduction

Photoemission electron microscopy (PEEM) is a powerful surface sensitive technique suitable for full field imaging of doping-induced contrast in semiconductors. In the energy filtered mode it combines high spatial and energy resolution allowing a comprehensive, non-destructive spectroscopic analysis to be carried out [1]. Correlation of the spatial distribution of core levels and valence band edges allows one to map chemical and valence band states. In PEEM a high extractor voltage, typically 12–20 kV, is applied between the sample and the entrance lens of the objective. The practical lateral resolution is determined by the counting statistics and the spherical and chromatic aberrations of the electron optics [2] while the ultimate resolution limit is given by the diffraction disk of the low energy electrons. In the vicinity of a planar pn junction (the junction being in a plane perpendicular to the optical axis), a lateral electric field is created, which alters the surface electrical topography and hence the PEEM image. The local field at a pn junction in silicon can easily be of the same order of magnitude as the extractor field. Electrons emitted from the surface in the physical vicinity of the junction are deviated laterally,

perturbing the PEEM image. Not only will the position of the junction as measured in PEEM be different from the real physical position, but also the apparent junction width may be modified. An understanding of the effect of the built-in voltage could therefore be used to measure the local lateral electric field at the junction from the PEEM image. The physical width of a high quality junction is much smaller than standard threshold PEEM resolution (typically 50 nm). However, the space charge of the depletion width can vary from several nm up to several microns depending on the doping levels. Therefore, these regions should provide a characteristic signal in the images as shown in some pioneering PEEM work on pn junctions [3]. The distortions in electron emission microscopy due to the doping dependent space charge region have been discussed by Frank et al. [4]. Potential mapping in semiconductor electronics by electron emission microscopy has been reviewed by Nepijko et al. [5]. The basic electron optic system considered is a cathode immersion lens and a contrast aperture or knife edge in the focal plane. The deviation of the electrons emitted from the surface was calculated analytically, modeled numerically and found to agree with imaging in bright and dark field modes. The built-in electric field across the pn junction deviates the electrons from the p-type region to the n-type region. The effect is shown schematically in Fig. 1. Typical values used for the simulations are an extractor field of 6.6 kV mm^{-1} and a built-in planar junction voltage of $\sim 0.9 \text{ V}$, giving an effective field vector influencing the photoelectron

* Corresponding author. Tel.: +33 169083272; fax: +33 169088446
E-mail address: nick.barrett@cea.fr (N. Barrett).

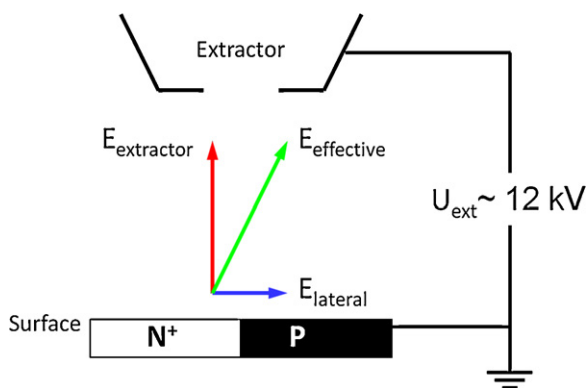


Fig. 1. Schematic of the perturbation of the extractor field by sample surface electrical topography in a cathode immersion lens.

trajectories starting at the surface. Away from the sample the effective field vector is less affected.

In real patterned samples electrical topography can combine with physical topography due to the patterning process. The focusing/defocusing effect of 3D structures has already been investigated in emission microscopy [6] and in mirror electron microscopy [7,8]. Dips or wells will tend to focus the photo-emitted (or reflected electrons in the case of low energy electron microscopy) whereas a protuberance will defocus them. Thus, close to a pn junction the field lines will be distorted due to a combination of the built-in field from the band line-up and the perturbation of the extractor field due to physical topography. Finally, the band line-up at the surface can be influenced by both the surface composition and the photoemission process. Native oxide can be removed and the surface passivated, however, residual oxide and defects may still be present, giving rise to band bending and pinning of the Fermi level. The generation of electron hole pairs during the photoemission process can also shift the band line-up via the surface photovoltage [9]. Thus although we are interested in the effect of the built-in voltage of the junction, the PEEM image may also be modified by surface effects. In this paper we investigate the combined effect of electrical and physical topography at pn junctions on PEEM imaging. First, the energy filtered threshold and Si2p PEEM measurements are presented. Then, the numerical model including an immersion lens and contrast aperture for the simulations is described and tested. Finally the simulations of the combined physical and electrical topography are compared with experiment and discussed.

2. Experiment

2.1. Sample preparation

The sample consisted of highly n-doped patterns (hereafter N^+) on a p-doped Si(100) substrate (resistivity 5–10 $\Omega\cdot\text{m}$), hereafter denoted P . Patterning was done by deep-UV photolithography with HF-last wet cleaning at 950 °C to remove native oxide. Cavities were etched using gaseous HCl (180 Torr, 750 °C). Cavity dimensions were adjusted to account for the isotropic etching below the thermal oxide. Epitaxial growth of boron and phosphorus doped silicon in the cavities was performed at 950 °C, 20 Torr using SiH_2Cl_2 , B_2H_6 and PH_3 gas precursors. Epitaxial growth was preferred to ion implantation in order to avoid collateral damage due to the ion energy and to minimize doping profiles creating sharp planar junctions. PEEM imaging was done on a “0”-shaped, P type pattern in a surrounding N^+ field. Prior to PEEM analysis, the surfaces were passivated using a three steps process to minimize surface band bending. After degreasing in trichloroethylene, rinsing in acetone and de-ionized water, a first etching was done using

a buffered oxide etchant (BOE: 49%, HF: 40%, NH_4F in a 7:1 ratio). The sample was then chemically oxidized using a Piranha solution (1/3 H_2O_2 , 2/3 H_2SO_4 , concentrations 30% and 96% respectively) for 20 min. The sample was re-etched in BOE for 30 min, dried under N_2 and immediately introduced into the PEEM vacuum system.

The N^+ doping level was measured with dual-beam time-of flight mass spectrometry using 1 keV Cs^+ sputtering to be 1.8×10^{19} atoms cm^{-3} , the as supplied substrate doping level was 1.4×10^{15} atoms cm^{-3} , creating a built-in voltage of 0.884 V at the planar pn junction. The space charge region on the N^+ side is estimated at 10 nm and on the P doped substrate at 540 nm. The localized epitaxial growth produced a physical topography at the junction because it was not possible to stop the epitaxial growth rate at exactly the same height as the top of the trench. Fig. 2 shows an AFM profile of the N^+/P structure and the height profile. The epitaxial N^+ grown in the trenches is 20 nm higher than the surrounding substrate.

Based on the AFM measurements and the measured doping levels we can represent the $P/N^+/P$ and $N^+/P/N^+$ structures as shown in Fig. 3(a). The space-charge region extends mainly into the P doped side of the junction whereas in the heavily N doped side it is almost negligible. Fig. 3(b) is a schematic of the expected effects of the real electrical and physical topographies on the electron trajectories. Both the built-in field due to the space-charge region and the step at the junction should modify the PEEM image, as shown schematically by the dark (purple) and light (yellow) field lines, respectively.

2.2. PEEM results

The optical micrograph in Fig. 4(a) shows the structure used for evaluation of the electrical topography. The N^+ structure is 7.65 μm wide, enclosed by the purple arrows. In this paper we focus on the $P/N^+/P$ structure. The dimension chosen is far from the center of the image because the N^+ structures at the center also undergo a charging effect due to photoemission which might influence the results. [10] The width of the structures was chosen to be much larger than the expected depletion width to ensure that accurate flat-band voltages far from the junctions were available both in the PEEM measurement and for the numerical simulations. The experiments were done using a spectroscopic XPEEM instrument (NanoESCA, Omicron Nanotechnology) temporarily installed at the TEMPO beamline of the SOLEIL synchrotron ($h\nu = 128.9$ eV). The double hemispherical analyzer used as energy filter provides high transmission and therefore allows spectroscopic imaging with high energy resolution without degrading the experimental lateral resolution [11]. The extractor voltage was set at 12 kV and the contrast aperture was closed down to 70 μm , giving a lateral resolution better than 70 nm. The overall energy resolution including the bandwidth of the photon beam was 0.1 eV for the threshold data, as measured at the Fermi level of a silver single crystal sample. The latter was also used to calibrate the photon energy.

Threshold image series were acquired as a function of the photoelectron energy referenced to the Fermi level, $E - E_F$. The take-off or kinetic energy is the difference between this value and the work function. A typical image is shown in Fig. 4(b). An image series acquired over the threshold spectrum gives a direct measurement of the sample work function in the field of view (FoV). Dark and flat field imaging eliminate camera noise and detector inhomogeneity, respectively. The non-isochromaticity [12] of the PEEM images was corrected by a parabolic function extracted from a uniformly doped sample area [13]. The pixel by pixel photoemission threshold spectra were fitted using a customized MATLAB routine by a complementary error function, providing a 2D workfunction map of the FoV with a standard deviation of ± 0.02 eV. The resulting work function map is presented in Fig. 4(d). The work function of the

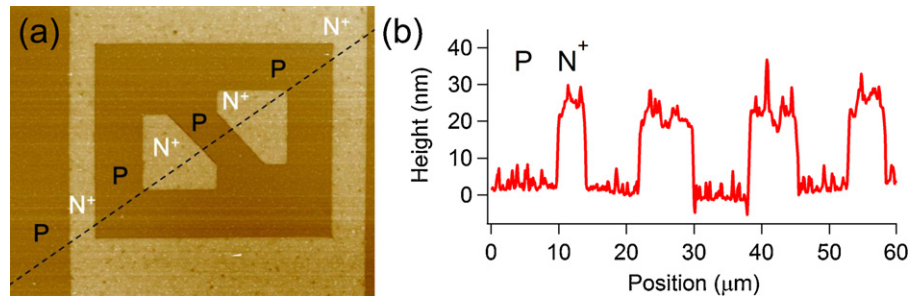


Fig. 2. (a) Atomic force microscopy image of the N^+/P structure and (b) height profile following the black line in (a). The N^+ region is 20 nm higher than the P substrate.

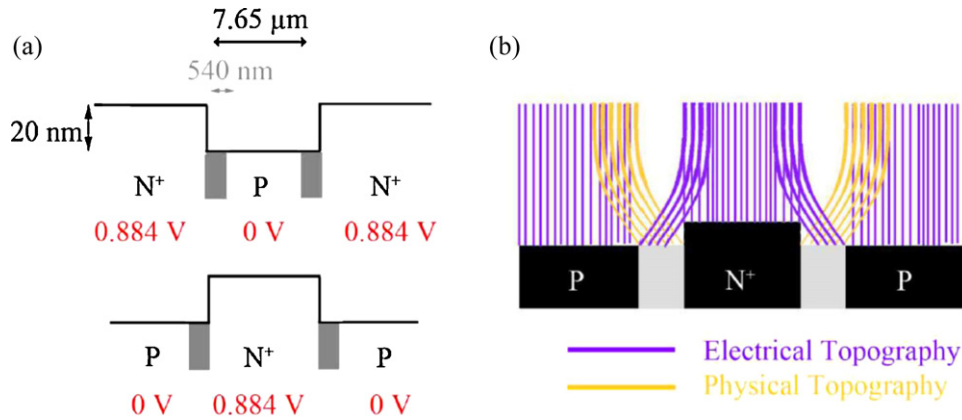


Fig. 3. (a) Schematic of real physical and electrical topographies of the $N^+/P/N^+$ (top) and $P/N^+/P$ (bottom) structures studied here and (b) schematic of the deviation of the electron paths predicted by the physical and electronic topographies of the $P/N^+/P$ structure. (For interpretation of references to color in the text, the reader is referred to the web version of this article.)

N^+ (P) region is 4.44 (4.38) eV. One would expect the N^+ region to have a lower work function, however, surface band bending and photovoltage can easily change this [14]. There is also contrast between open and closed N^+ regions due to biasing of the

pn junction under photoemission that has already been discussed [10]. The Si 2p image series was also acquired using the same photon energy. A typical image ($E_0 - E_F = 30.50$ eV, corresponding to a kinetic energy of 26.0 eV) is shown in Fig. 4(c).

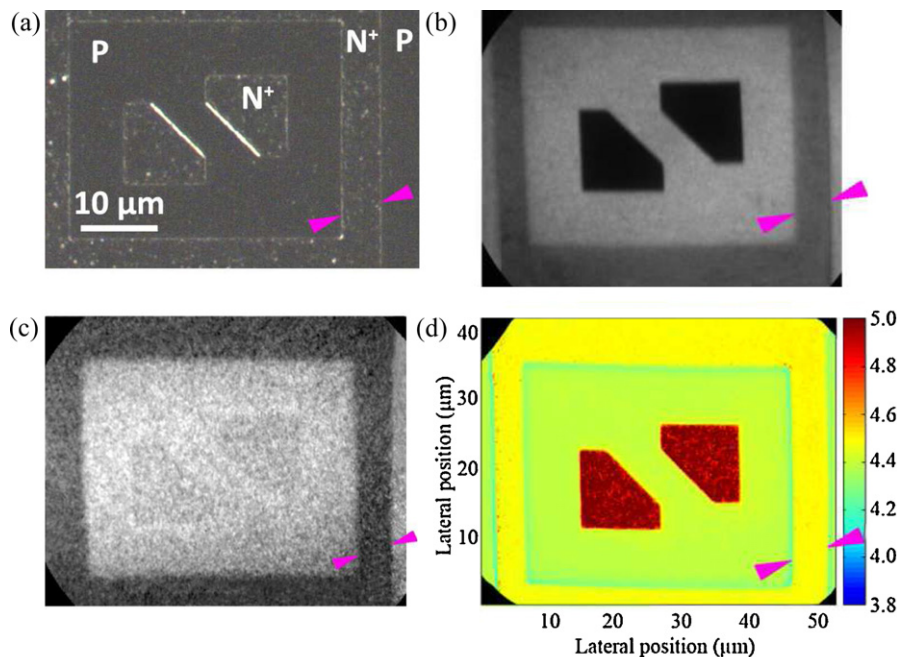


Fig. 4. (a) Optical micrograph of N^+/P silicon sample showing the micron scale doped pattern used in this work, (b) typical energy filtered threshold PEEM image for a take-off energy of 0.1 eV, (c) energy filtered image at the Si 2p core level ($h\nu = 128.9$ eV, $E - E_F = 26.0$ eV) and (d) work function map obtained from a pixel by pixel complementary error function fit to the local threshold spectra. (For interpretation of reference to color in the text, the reader is referred to the web version of this article.)

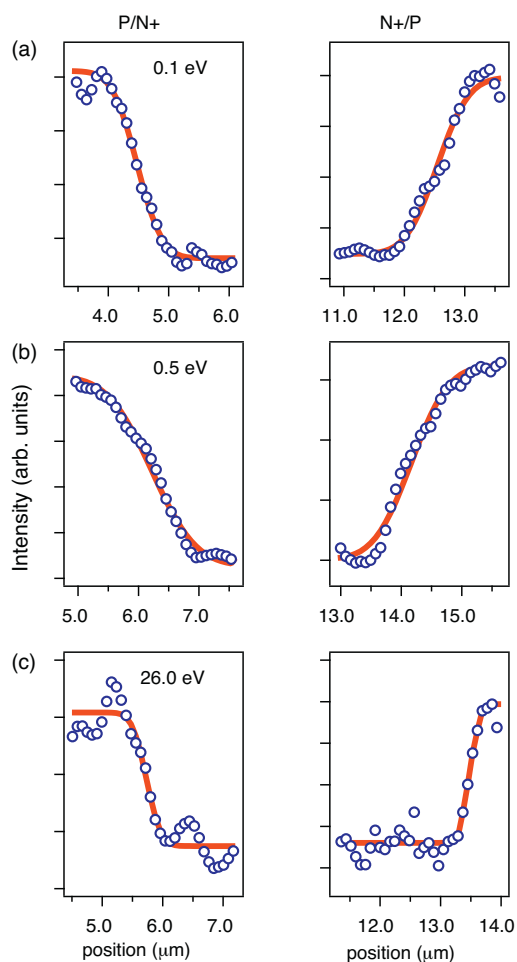


Fig. 5. Intensity profiles (blue circles) of the left and right hand junctions of P/N⁺/P structure at take-off energies of (a) 0.1 eV, (b) 0.5 eV and (c) 26.0 eV. Error function fits to the profile are shown as red lines. The take-off energy is measured with respect to the vacuum level E_0 of the N⁺ region. (For interpretation of references to color in this figure legend, the reader is referred to the web version of this article.)

To measure the width of the P/N⁺/P structure complementary error functions have been used to fit the intensity profiles of the left and right hand junctions. The results are shown in Fig. 5. The widths, as deduced from the fits in Fig. 5 are (a) 7.95, (b) 7.82 and (c) 7.65 μm for take-off energies of 0.1, 0.5 and 26.0 eV, respectively. Thus, the width of the structure as determined from the intensity profile at the Si 2p core level gives an identical value to that of the optical micrograph, whereas the measurements at threshold give significantly larger values, in agreement with the behavior shown in the schematic of Fig. 3(b). The built-in field sweeps electrons towards the n-type regions, reducing the intensity from the p-type region near the junction. A width measurement based on the intensity profile will therefore give a larger value than the actual physical width. However, this behavior needs to be quantified, both in terms of electrical and physical topography and is the aim of the simulations presented in the next section.

3. Simulations

3.1. Model

The PEEM contrast observed at the junction has been numerically simulated using the standard industry code SIMION [15] which traces the motion of charged particles in an electric field using a fourth-order Runge–Kutta integrator. We have

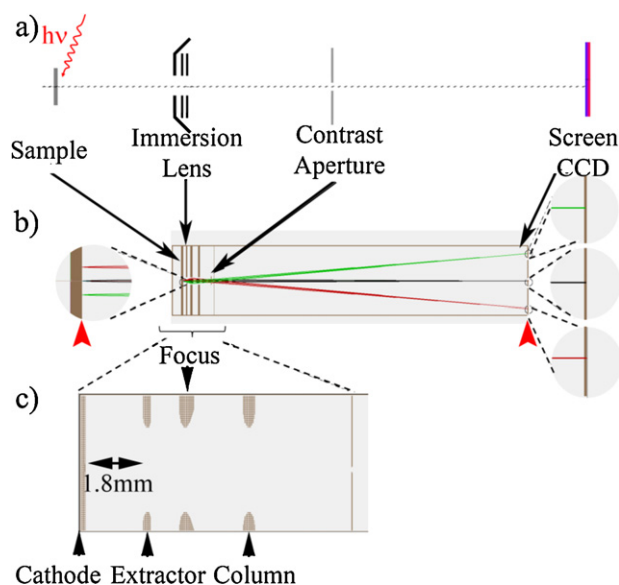


Fig. 6. Electron optics model used to simulate the real PEEM optics: (a) PEEM optical elements, (b) SIMION overview of electron paths and (c) zoom on the PEEM first elements included in the simulations. The red arrows show the position of the planes used to image the simulated electron densities. (For interpretation of references to color in this figure legend, the reader is referred to the web version of this article.)

approximated the PEEM by a sample (the cathode), a single electrostatic lens, a contrast aperture in the focal plane and the screen, as shown in Fig. 6. Energy filtering is obtained by defining the take-off energy of the photoelectrons. Although the electron optics are simplified compared to the NanoESCA instrument (notably two projective lenses, a transfer lens and analyzer entrance and exit slits should be added), they do reproduce the essential characteristics of an energy filtered PEEM with a contrast aperture in the focal plane. Caustic effects, observed in low energy electron microscopy, are not included, i.e. we assume only deviations in the plane perpendicular to the optical axis [8]. This is reasonable since the energy filtering prevents simultaneous imaging of photoelectrons in a bandwidth greater than the energy resolution of the PEEM.

The electrons are simulated by an array of point sources distributed across the sample surface; each point source has 11 different starting angles from -10° to $+10^\circ$ in 2° steps. The built-in potential due to the pn junction is simulated by an array of linear voltage drops across the depletion width. The central P or N⁺ region was 7.65 μm wide, corresponding to the optically determined width. The electron intensity distribution can be extracted at any plane perpendicular to the electron optical axis, in particular just above the sample surface and at the screen position as indicated by the thick (red) arrows in Fig. 6(b). This allows determination of the influence of the contrast aperture on the intensity distribution in the PEEM image. To test of the validity of our electron optics we have calculated the magnification of the PEEM simulation as a function of take-off energy, i.e. electron kinetic energy, defined as the electron energy above threshold, measured experimentally. The results are plotted in Fig. 7 and compared, using a linear scaling factor, to the calculated magnification of the PEEM optics (solid line).

These initial simulations only take account of the effect of the built-in voltage across the junction and the electron optics of the PEEM column. They do not simulate, for example, the photoelectron yield. An empirical correction for this effect will be introduced below. Furthermore, the work function varies slightly between N⁺ and P regions, the simulation of a PEEM image taken at a fixed $E - E_F$ value therefore requires the use of different photoelectron take-off energies.

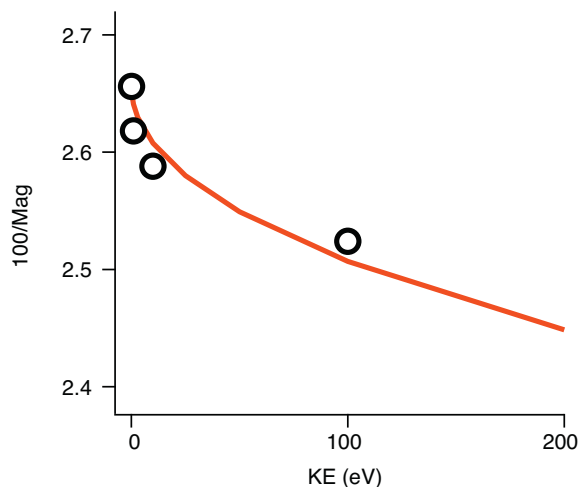


Fig. 7. Simulated magnification (circles) obtained using the simplified imaging column compared, using a linear scaling factor, with the calculated magnification (solid line) of the full PEEM electron optics as a function of kinetic energy.

3.2. Results

As a first step we calculate the deviation of the electrons due to the lateral electric field and the physical topography, without taking into account take-off energy differences or electron yield. In Fig. 8 we show the simulated electron intensity of the $N^+/P/N^+$ and $P/N^+/P$ structures in a plane just above the sample and as measured on the screen, i.e. in the positions defined by the red arrows in Fig. 6(b). A five point nearest neighbor smoothing is done to the simulated raw data. As intuitively expected, electrons are deviated from the p-type region near the junction to reinforce the intensity on the n-type side in both cases. This gives rise to a dark stripe on the p-type side with an adjacent bright stripe in the PEEM image of the junction without the contrast aperture, as previously observed and predicted numerically [16]. The introduction of a realistic contrast aperture centered in the focal plane with respect to the electron optical axis acts as an angular selector and cuts off strongly deviated electrons. We have used a $70\ \mu\text{m}$ contrast aperture which gives a high spatial resolution as required in the experiment. The intensity distribution observed on the screen modifies considerably with respect to that in the absence of a contrast aperture, as can be seen from the darker (blue and red) curves in Fig. 8. The major effect of the contrast aperture is to suppress the bright stripe

due to highly deviated electrons; however, it also displaces the dark stripe further into the P doped region. In fact, with or without the contrast aperture it is difficult to accurately measure the junction position.

The cut-off effect of the contrast aperture has been checked experimentally. We show in Fig. 9 threshold images of the same structure with a $70\ \mu\text{m}$ contrast aperture in centered and off center positions with respect to the electron optical axis of the PEEM column. The intense signal due to the highly deviated electrons is cut by the centered contrast aperture whereas in the off center positions there is almost a perfect symmetry, with the bright lines observed in the N doped regions. These images were obtained on a P^+/N patterned sample, but as can be deduced from the simulations in Fig. 8 this does not qualitatively change the cut-off of the highly deviated electrons by the contrast aperture. The simulations therefore reproduce qualitatively the experimental deviation of the photoemitted electrons by the built-in junction field. For the comparison of the simulations with experiment, we focus on the $P/N^+/P$ structure. In order to evaluate the effect of the physical topography we have repeated the simulations of Fig. 8 for the $P/N^+/P$ structure with and without the experimentally measured step of $20\ \text{nm}$. The results are shown in Fig. 10(a) for the electron density just above the sample and in Fig. 10(b) for electron intensity on the screen with the contrast aperture in place.

From Fig. 10(a) the physical and electrical topographies work in opposite directions. The bright stripe due to the built-in electric field is inside the N^+ area, whereas for only a physical height difference of $20\ \text{nm}$ at the junction a bright stripe is created on the P side of the junction. On the screen (Fig. 10(b)) the contrast aperture has cut off the highly deviated electrons at the origin of these stripes and we see that the modification of the PEEM image is due, in this case, principally to the built-in electric field, although the variation in the intensity profile across the junction is partially compensated by the physical topography. In the following we will therefore consider only the effect of the built-in electric field although it should be borne in mind that larger height differences at a junction would significantly affect the measurement of the structure width. As can be seen from Fig. 8 in the presence of a contrast aperture, the bright deviated intensity is suppressed and there is a dip in the intensity on the screen inside (outside) the central P (N^+) structure. The physical junction position is close to the outer (inner) edge of this dip respectively. Thus, depending on the criterion used experimentally to position the junction, the measured width will be different. For example, if the outside edge

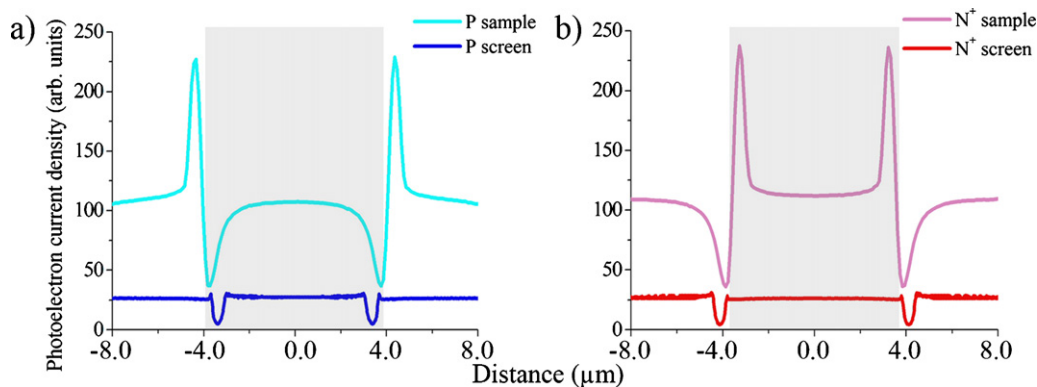


Fig. 8. Simulated photoelectron density emitted from the sample surface (light blue and red lines) and on the PEEM screen after passing through the contrast aperture (dark lines) for the (a) $N^+/P/N^+$ and (b) $P/N^+/P$ structures. The pattern dimensions on the screen are given with respect to the sample surface using the PEEM objective magnification. The contrast aperture suppresses the bright stripe due to highly deviated electrons and displaces the low one. (For interpretation of references to color in this figure legend, the reader is referred to the web version of this article.)

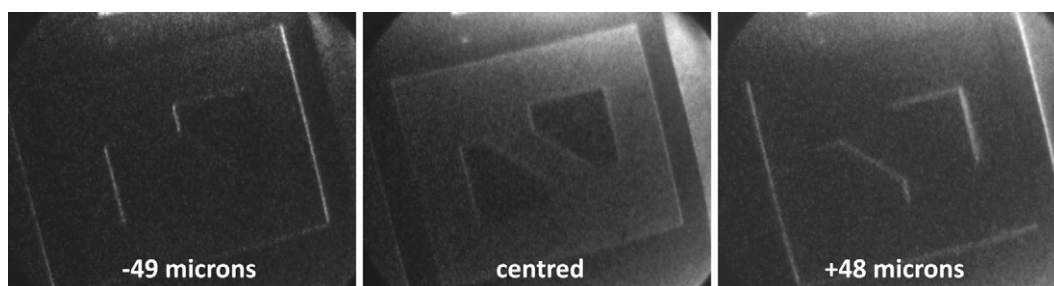


Fig. 9. Bright and dark field PEEM images of a P^+/N sample obtained by varying the position of the contrast aperture. When the contrast aperture is off-center with respect to the optical axis, the bright stripe due to the deviated electrons becomes clearly visible.

of the dip is used then the structure width will appear larger than the real physical width. These simulations used to compare with the experimental results take into account the intensity differences by empirically including a gradient of the number of photoelectrons across the depletion region for each take-off energy. The intensity from the P region is always greater than that from the N^+ region in the images used for comparison with the simulations. We have therefore arbitrarily set the higher, P intensity at twice the number of particles (108 every 10 nm) in the range of $-10^\circ/+10^\circ$ as the lower N^+ intensity emission (54 particles every 10 nm in the range of $-10^\circ/+10^\circ$). Note that we assume that the lateral electric field due to the built-in junction voltage is determined by the relative doping levels whereas the take-off energy is measured with respect to the experimentally determined threshold energy.

The simulated profiles, taking into account the built-in field, physical topography and the different levels of intensity in the P

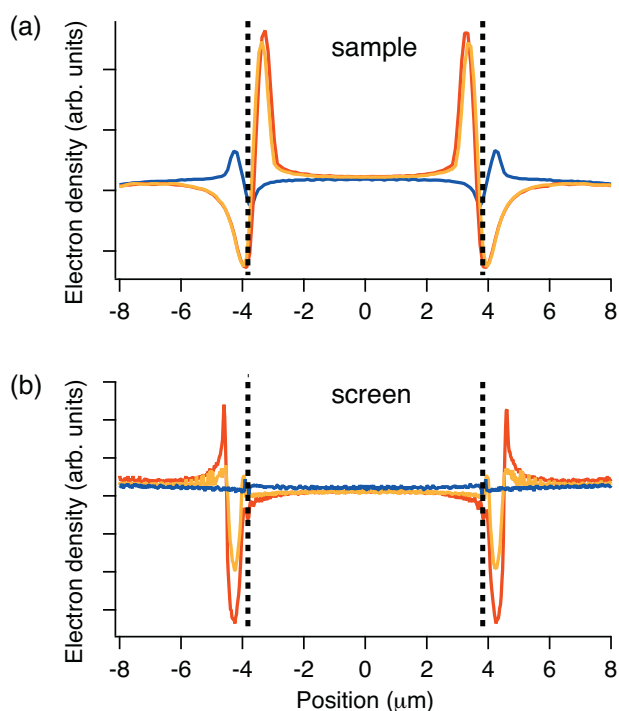


Fig. 10. Simulated photoelectron intensity emitted from (a) the sample surface and (b) on the PEEM screen after passing through the contrast aperture for the $P/N^+/P$ structure with physical (blue), electrical (orange) and physical and electrical topographies (red) topography. A take-off energy of 0.1 eV was used. The contrast aperture suppresses the bright stripes due to highly deviated electrons. The simulated profile near the sample surface (a) shows that physical and electrical topographies work in opposite directions whereas the screen profile shows that in this case, the electrical topography dominates the distortion of the PEEM image. (For interpretation of references to color in this figure legend, the reader is referred to the web version of this article.)

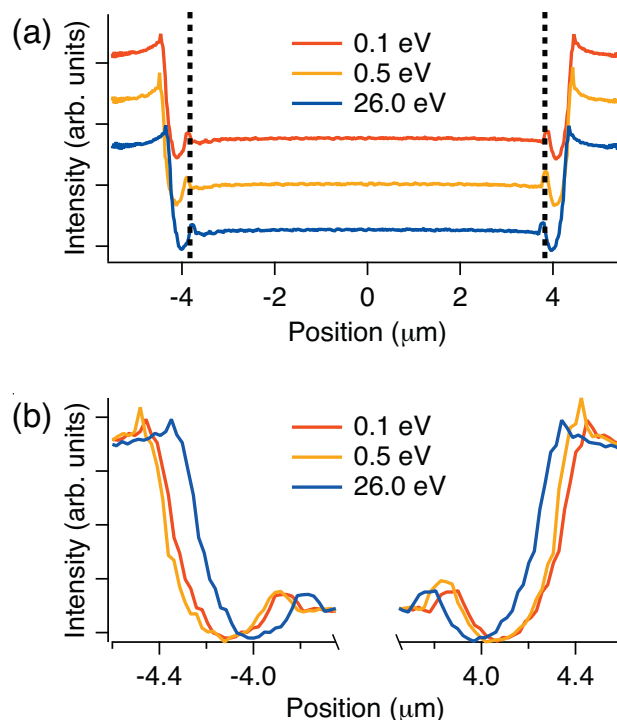


Fig. 11. (a) Simulated intensity profiles at take-off energies of (from top to bottom) 0.1, 0.5 and 26.0 eV of the $P/N^+/P$ structure. The vertical dotted lines represent the real junction position as determined from optical microscopy. Simulations include variation in the take-off energy across the junction, 20 nm physical topography and varying electron yield defined by the measured threshold shift and (b) close-ups of the simulated intensity profiles across the left (P/N^+) and right (N^+/P) hand junctions in (a).

and N^+ regions via a gradient of emitted particles are shown in Fig. 11(a) for 0.1, 0.5 and 26.0 eV. The vertical dotted lines indicate the junction position as measured by optical microscopy. The lower panel shows close-ups of the simulated intensity profile across the left and right hand junctions. As the take-off energy increases, the effective width of the N^+ central structure as measured from the intensity profile decreases, in agreement with the experimental data. These more sophisticated simulations at threshold confirm the position of the intensity dip with respect to the physical junction position seen in Fig. 8. The apparent width of the structure, as determined from a fit to the fastest changing part of the intensity profile, shrinks by $0.35 \mu\text{m}$ between a take-off energy of 0.1 eV and 26.0 eV. The change in the apparent width is of the same order as the depletion region on the P side and two orders of magnitude greater than the depletion region on the N^+ side of the junction. For the Si 2p profile (take-off energy 26 eV) the edges of the intensity profile of the central N^+ region coincide with the real junction position.

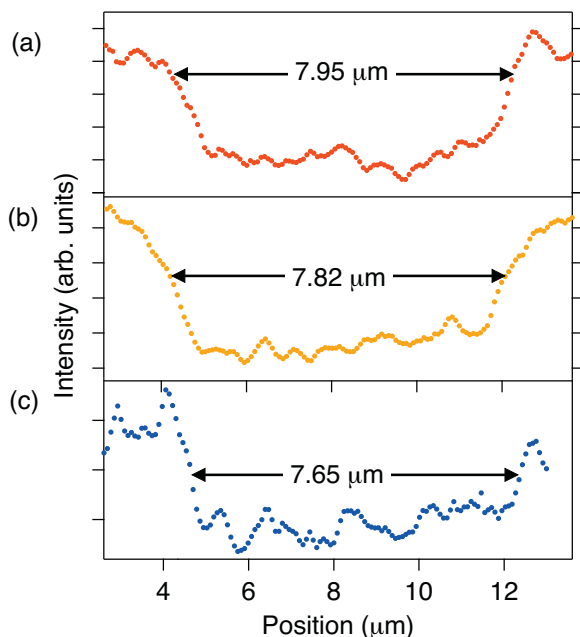


Fig. 12. Full experimental intensity profiles at take-off energies of (a) 0.1, (b) 0.5 and (c) 26.0 eV of the P/N⁺/P structure used to obtain the profiles in Fig. 5. The width of the N⁺ region as found from the error function fits in Fig. 5 is indicated in each case.

4. Discussion

Fig. 12 shows the whole experimental intensity profiles used for the fits in Fig. 5. The experimental profile across the junction is much broader than in the simulation. This may be due to the fact that the experimental energy resolution, 0.1 eV, is the same as the lowest take-off energy considered. Low take-off energy electrons are expected to be the most sensitive to lateral fields across the junction [6]. The finite band pass means that in the experiment electrons with take-off energies varying over approximately 0.1 eV are recorded in the same image. There will therefore be a spread in the deviation of the electrons by the built-in field, broadening the intensity profile measured across the junction. The effect of the experimental resolution can be seen in Fig. 13. We show two images from the threshold series, Fig. 13(a) is recorded at the value of the N⁺ work function (4.44 eV) whereas Fig. 13(b) is the image obtained at 4.24 eV. The doped regions are dark but there are still bright stripes from near the junctions. $E_0 - E_F = 4.24$ eV is more than twice the energy resolution below the work function so that the image should be uniformly dark. However, photoelectrons

deviated by the built-in field at the junction will have an effective take-off energy lower than electrons emitted far from the junction. They will therefore be imaged at lower $E - E_F$, which is what we observe. The work function map also shows electron emission at lower $E - E_F$. Note that this cannot be due to field-enhanced emission due to the 20 nm step between the P and the N⁺ regions since it is not present at the junction between the inner N⁺ region and the P region. Very low energy electrons are therefore doubly unsuitable for direct measurements of doped pattern dimensions. On the one hand they are the most strongly affected by the built-in field, and on the other hand, if the energy resolution is similar to the take-off energy, there will be an additional spread of the electron paths.

The width of the central structure approaches the real physical value of 7.65 μm for 26.0 eV. However, unfortunately, the signal to noise ratio of the intensity profile at 26.0 eV is also much lower. This is to be expected for PEEM imaging of a core level with respect to threshold electrons. A more accurate measurement therefore requires not only high take-off energy but also much longer counting time in order to obtain a reliable value. It should be emphasized that the differences observed in the measurement of the junction position are absolute values. They do not depend on the width of the structure itself but on the value of the built-in field across the junction, in other words, on the relative doping levels on either side of the junction. At threshold, the difference is 0.3–0.4 μm . Thus, if much smaller structures are to be imaged, the difference can be as big or even bigger than the dimensions of interest.

As an illustration of this, we have imaged a different sample with a much narrower structure consisting of two 100 nm wide N⁺ stripes 100 nm apart on a P type substrate (Fig. 14(a)). Fig. 14(b–f) shows threshold images of the structure. Contrast inversion is observed between the outlying p-type substrate and the central region containing the n-type stripes. More importantly, however, apart from the image acquired for $E - E_F = 4.95$ eV, the P type band separating the two N⁺ stripes is invisible in the PEEM image. This is confirmed by the local threshold spectra in Fig. 14(g) extracted from the regions of interest across the structure. Whereas the photoemission threshold typical of the P type substrate is clearly visible far from the structure, at the center a double threshold is observed corresponding to electrons emitted from both P and N⁺ patterns. It is therefore impossible to resolve the central P band because of the built-in field. This is independent of the lateral resolution of the PEEM which is better than 70 nm. In this case, the N⁺ and P doping levels are 10^{20} and 10^{15} atom cm^{-3} , respectively, corresponding to a built-in voltage of 0.914 V and a space charge region 1.10 μm wide. In fact, the central P structure is fully depleted and the structure acts as a 300 nm N⁺ stripe for imaging. Most patterns will fall between the two extremes illustrated here. When using threshold electrons great care must be taken in order to deduce

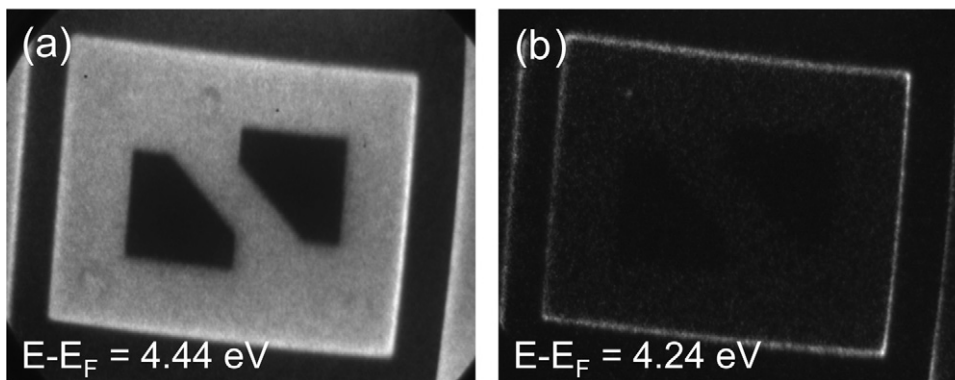


Fig. 13. Threshold PEEM images recorded at (a) $E - E_F = 4.44$ eV (the work function value) and (b) $E_0 - E_F = 4.24$ eV showing that the intensity at $E - E_F$ below the work function is due to deviated electrons with a lower effective kinetic energy as measured in PEEM. The energy resolution is 0.1 eV.

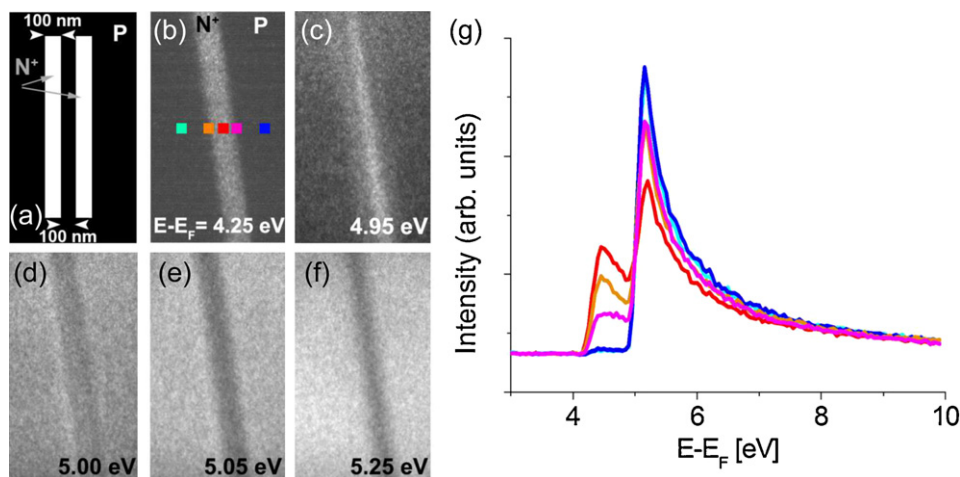


Fig. 14. (a) Structure composed of 100 nm N^+ and P stripes, (b–f) samples of the threshold image series showing that the structure reacts as a 300 nm N^+ stripe in imaging mode and (g) threshold spectra extracted from image series. The double threshold for the local spectra of the stripe structure shows the contribution of electrons from both P and N^+ regions.

dimensions in the presence of structures with an built-in lateral field. This will be the case for almost all patterned semiconducting samples. More generally, any potential asymmetry will give rise to a lateral field. For example, at ferroelectric domain walls there can be a strong lateral field induced by surface charge of opposite sign, proportional to the polarization difference between two domains. From the simulations it is apparent that take-off energies of more than a few eV (here 26.0 eV) are sufficient to minimize the effect of built-in fields. One method could be to systematically image the same structure as a function of take-off energy to determine the value at which the apparent size no longer changes. Deviation of the electron paths by an built-in lateral field could also be used to measure the field strength. This would require a complete electron optic simulation of the PEEM instrument. In the present simulations we have used realistic sample-to-objective distance, objective lens, contrast aperture and PEEM magnification. These appear sufficient to reproduce the essential behavior of the low energy electrons. A more quantitative approach would require simulation of the full PEEM optics, including the effect of the analyzer entrance slit and pass energy, in other words, the phase space loss between the PEEM column and the energy analyzer. The method could then be applied to measure surface doping levels and hence the depletion width of a pn junction, as discussed recently using the secondary electron signal from a scanning electron microscope [17].

5. Conclusions

We have carried out a quantitative study of the effect of electrical and physical topography on the width of N^+ and P type regions in a P/ N^+ /P structure as measured by PEEM. At threshold the experimentally determined widths are significantly larger than the real physical width. As the take-off energy increases, the measured width decreases. At 26.0 eV an intensity profile of the PEEM image gives an accurate measurement of the structure. We have simulated the PEEM cathode lens, and included the experimentally determined built-in voltages and physical topography of the sample. Depending on the sign of the latter, the two contributions can act in the same or in opposite directions on the PEEM measured dimensions. The N^+ region is 20 nm higher than the P substrate giving a topography which acts in the opposite sense to the built-in field at the junction but does not qualitatively change the trend in structure width as measured by PEEM. Knowledge of the physical topography and one of the doping levels could be used to determine the surface doping level on the other side of the junction. These

conclusions could be extended to the more general case of any electrical asymmetry imaged by PEEM, for example, a Schottky barrier or ferroelectric domain wall. More detailed simulations could include both the intensity and the shape of the threshold spectra, for example using Henkes model for the secondary electron tail [18]. At low take-off energies, high spectroscopic resolution is mandatory. For a fully quantitative model of PEEM imaging of structures with lateral electric fields, electron optics simulations should include the full PEEM column and the energy filter.

Acknowledgments

We thank FOCUS GmbH for company data on the PEEM optics. M.L. benefited from a CEA Ph.D. grant. The work was supported by the French National Research Agency (ANR) through the Recherche Technologique de Base (RTB) program, and was partly performed in the Minatec Nanocharacterization Centre. We thank SOLEIL for provision of SR facilities and the TEMPO staff for their help.

References

- [1] R.J. Phaneuf, H.-C. Kan, M. Marsi, L. Gregoratti, S. Günther, M. Kiskinova, *J. Appl. Phys.* 88 (2) (2000) 863, <http://dx.doi.org/10.1063/1.373748>, <http://link.aip.org/link/JAPIAU/v88/i2/p863/s1&Agg=doi>
- [2] A. Bailly, O. Renault, N. Barrett, T. Desruets, D. Mariolle, L.F. Zagone, M. Escher, *J. Phys. Condens. Matter: Inst. Phys. J.* 21 (31) (2009) 314002, <http://www.ncbi.nlm.nih.gov/pubmed/21828563>
- [3] M. Giesen, J. Phaneuf, E.D. Williams, T.L. Einstein, *Surf. Sci.* 396 (100) (1998) 411–421.
- [4] L. Frank, I. Müllerová, D.A. Valdaitsev, A. Gloskovskii, S.A. Nepijko, H.-J. Elmers, G. Schönhense, *J. Appl. Phys.* 100 (9) (2006) 093712, <http://link.aip.org/link/JAPIAU/v100/i9/p093712/s1&Agg=doi>
- [5] S.A. Nepijko, N.N. Sedov, G. Schönhense, M. Escher, *J. Microsc.* 206 (Pt 2) (2002) 132–138, <http://www.ncbi.nlm.nih.gov/pubmed/12000552>
- [6] S. Nepijko, N.N. Sedov, O. Schmidt, G. Schönhense, X. Bao, W. Huang, *J. Microsc.* 202 (Pt 3) (2001) 480–487, <http://www.ncbi.nlm.nih.gov/pubmed/11422670>
- [7] H.-C. Kan, R.J. Phaneuf, *J. Vacuum Sci. Technol. B: Microelectron. Nanometer Struct.* 19 (4) (2001) 1158, <http://link.aip.org/link/JVTBD9/v19/i4/p1158/s1&Agg=doi>
- [8] S.M. Kennedy, C.X. Zheng, W.X. Tang, D.M. Paganin, D.E. Jesson, *Ultramicroscopy* 111 (5) (2011) 356–363, <http://www.ncbi.nlm.nih.gov/pubmed/21334287>
- [9] M.H. Hecht, *Phys. Rev. B* 41 (11) (1990) 7918–7922.
- [10] M. Lavyssière, O. Renault, D. Mariolle, M. Veillerot, J.P. Barnes, J.M. Hartmann, J. Leroy, N. Barrett, *Appl. Phys. Lett.* 99 (20) (2011) 202107, <http://link.aip.org/link/APPLAB/v99/i20/p202107/s1&Agg=doi>
- [11] M. Escher, N. Weber, M. Merkel, C. Ziethen, P. Bernhard, G. Schönhense, S. Schmidt, F. Forster, F. Reinert, B. Krömker, D. Funnemann, *J. Phys.: Condens. Matter* 17 (16) (2005) S1329–S1338, doi:10.1088/0953-8984/17/16/004.
- [12] M. Escher, K. Winkler, O. Renault, N. Barrett, *J. Electron Spectrosc. Relat. Phenom.* 178–179 (2010) 303–316, doi:10.1016/j.elspec.2009.06.001.

- [13] F. de la Peña, N. Barrett, L.F. Zagonel, M. Walls, O. Renault, *Surf. Sci.* 604 (19–20) (2010) 1628–1636, doi:10.1016/j.susc.2010.06.006.
- [14] N. Barrett, L.F. Zagonel, O. Renault, a. Bailly, *J. Phys. Condens. Matter: Inst. Phys. J.* 21 (31) (2009) 314015, <http://www.ncbi.nlm.nih.gov/pubmed/21828576>
- [15] S.I.S. Inc. SIMION 3d. <http://simion.com/>
- [16] S.A. Nepijko, A. Gloskovskii, N.N. Sedov, G. Schönhense, *J. Microsc.* 211 (2003 April) 89–94.
- [17] J.T. Heath, C.-S. Jiang, M.M. Al-Jassim, *J. Appl. Phys.* 111 (4) (2012) 046103, <http://link.aip.org/link/JAPIAU/v111/i4/p046103/s1&Agg=doi>
- [18] B.L. Henke, J.A. Smith, D.T. Attwood, *J. Appl. Phys.* (1977) 1852, <http://link.aip.org/link/JAPIAU/v48/i5/p1852/s1&Agg=doi>.